

MAJOR PAPER

MR Imaging-based Evaluation of Mesenteric Ischemia Caused by Strangulated Small Bowel Obstruction and Mesenteric Venous Occlusion: An Experimental Study Using Rabbits

Akitoshi Inoue^{1*}, Norihisa Nitta¹, Shinichi Ota¹, Kai Takaki¹,
Yugo Imai¹, Sayaka Misaki¹, Takayasu Iwai¹, Akinaga Sonoda¹,
Ken-Ichi Mukaisho², and Kiyoshi Murata¹

Purpose: This study assessed the MRI findings of strangulated small bowel obstruction (SBO) and mesenteric venous occlusion (MVO) in a rabbit model using 3T MRI.

Materials and Methods: Twenty rabbits were included in this study. The strangulated SBO and MVO models were generated via surgical procedures in nine rabbits, and sham surgery was performed in two rabbits. The success of generating the models was confirmed via angiographic, macroscopic, and microscopic findings after the surgical procedure. MRI was performed before and 30 min after inducing mesenteric ischemia. T₁-weighted images (T₁WIs), T₂-weighted images (T₂WIs), and fat-suppressed T₂WIs (FS-T₂WIs) were obtained using the BLADE technique, and fat-suppressed T₁WIs (FS-T₁WIs) were obtained. The signal intensities of the affected bowel before and after the surgical procedures were visually categorized as high, iso, and low intense compared with the findings for the normal bowel wall on all sequences. Bowel wall thickness was measured, and the signal intensity ratio (SI ratio) was calculated using the signal intensities of the bowel wall and psoas muscle.

Results: Angiographic, macroscopic, and microscopic findings confirmed that all surgical procedures were successful. The ischemic bowel wall was thicker than the normal bowel. The bowel wall was thicker in the MVO model (3.17 ± 0.55 mm) than in the strangulated SBO model (2.26 ± 0.46 mm). The signal intensity and SI ratio of the bowel wall were significantly higher after the procedure than before the procedure on all sequences in both models. The mesentery adjacent to the ischemic bowel loop exhibited a high signal intensity in all animals on FS-T₂WIs.

Conclusion: Non-contrast MRI can be used to evaluate mesenteric ischemia caused by strangulated SBO and MVO. FS-T₂WIs represented the best modality for depicting the high signal intensity in the bowel wall and mesentery caused by ischemia.

Keywords: *mesenteric venous occlusion, rabbits, strangulated small bowel obstruction*

Introduction

Acute mesenteric ischemia is a life-threatening condition with a high mortality rate despite the development of diagnostic

and therapeutic strategies.¹ The unfavorable prognosis is associated with the difficulty in diagnosing the condition at an early stage. Primary acute mesenteric ischemia is caused by mesenteric arterial thrombosis, mesenteric arterial embolism, mesenteric venous thrombosis, or non-occlusive mesenteric ischemia, and secondary acute mesenteric ischemia results from strangulated small bowel obstruction (SBO).² Contrast-enhanced CT plays a pivotal role in diagnosing acute mesenteric ischemia and contributes to improving the prognosis of acute mesenteric ischemia;³ however, imaging modalities lacking ionizing radiation exposure are ideal for pregnant females and children.⁴ Intravenous administration of iodine contrast medium is avoided in patients with renal dysfunction or those with contraindications to iodine contrast

¹Department of Radiology, Shiga University of Medical Science, Seta Tsukinowacho, Otsu, Shiga 520-2145, Japan

²Division of Molecular and Diagnostic Pathology, Shiga University of Medical Science, Shiga, Japan

*Corresponding author, Phone: +81-77-548-2288, Fax: +81-77-548-2536, E-mail: akino@belle.shiga-med.ac.jp

©2019 Japanese Society for Magnetic Resonance in Medicine

This work is licensed under a Creative Commons Attribution-NonCommercial-NoDerivatives International License.

Received: January 24, 2019 | Accepted: March 30, 2019

medium such as anaphylaxis.⁵ Consequently, delays in diagnosis can lead to massive bowel necrosis and death. Actually, we encountered a patient with chronic renal failure who suffered from acute mesenteric ischemia and was not diagnosed immediately. This was because we hesitated to administrate iodine contrast media to avoid contrast-associated acute kidney injury, and finally, the massive small bowel was removed a day after administration. Conversely, MRI can provide diagnostic images without exposure to ionizing radiation exposure or administration of contrast agents. A recent study reported that exposure to MRI without a gadolinium-based contrast agent during the first trimester of pregnancy was not associated with adverse events in the child either during pregnancy or in early childhood compared with the findings for non-exposure.⁶ Consequently, MRI is recommended for acute abdominal pain in pregnant patients.^{7,8} The use of MRI in patients with acute abdominal pain was previously limited to patients with biliary and gynecological disease that could not be diagnosed using CT; however, several studies reported that MRI is helpful for diagnosing acute abdominal pain caused by not only acute appendicitis^{9–12} but also other diseases.^{13–15} MRI has potentially high-contrast resolution, and it can illuminate ischemic changes caused by acute mesenteric ischemia. In several animal experiments, strangulated SBO, mesenteric arterial ischemia, and mesenteric venous ischemia were assessed using a 7T micro MRI scanner, which is not available in the clinical setting.^{16–18} A few articles reported the evaluation of mesenteric arterial ischemia using rabbit or pig models and clinically available MRI modalities such as 3T MRI^{19–21}; however, mesenteric venous ischemia and strangulated SBO were not evaluated in animal experiments using clinically available MRI systems. This study thus aimed to assess the MRI findings of strangulated SBO and mesenteric venous occlusion (MVO) in a rabbit model using 3T MRI.

Materials and Methods

Animal models

All procedures performed in studies involving animals were conducted in accordance with the ethical standards of practice of the institution where the studies were conducted. Our study protocol was approved by the Animal Experimentation Committee of our institute, and all experiments were performed according to its Animal Care Guidelines. We used 20 female Japanese white rabbits (age: 14–16 weeks, body weight: 2.87 ± 0.12 kg), which were bred without any special feed carried from the animal breeding company (KITAYAMA LABES CO., LTD, Nagano, Japan) in this study. The diet was not restricted before procedure. General anesthesia was administrated intramuscularly to each rabbit using a combination of ketamine hydrochloride (20 mg/kg body weight; Ketalar, Daiichi Sankyo, Tokyo, Japan) and dexmedetomidine hydrochloride (0.1 mg/kg body weight; Domitor, Zenoac, Fukushima, Japan). Their

extremities were bound to a board while they were in a supine position. The temperature in the experimental room was maintained at 25°C using an air conditioner, even though the body temperature of rabbits was not measured during the procedure.

Mesenteric ischemia rabbit model

We induced strangulated SBO in nine rabbits. First, we cut the abdominal wall and brought the small bowel and mesentery outside the body. We ligated the small bowel, with its mesentery at one point, using a thread to create a closed loop involving approximately 30 cm of the small intestine (Fig. 1). After that, we put the small intestine and mesentery back into the abdominal cavity and closed the abdominal wall.

In the other nine rabbits, we induced venous occlusion. We approached the small bowel and mesentery as described for strangulated SBO. We made a small hole in the mesentery using a 23-gauge needle and ligated the three branches of the mesenteric vein and both ends of the marginal vein using a thread (Fig. 2). We placed a marker in the ischemic mesentery to identify the ischemic lesion in both models. Surgical procedure took approximately 15 min.

In the remaining two rabbits, we performed sham surgery. We cut through the abdominal wall, brought the small bowel

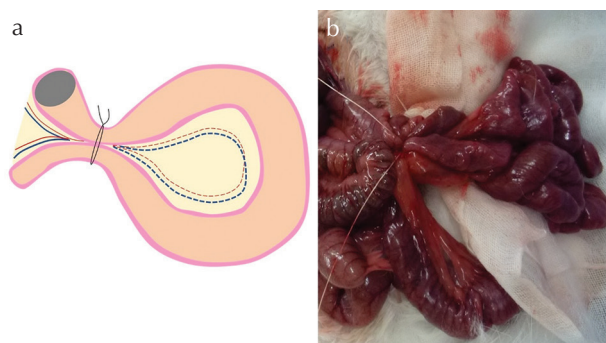


Fig. 1 Surgical procedure to induce a strangulated small bowel obstruction (SBO). The small bowel with its mesentery is ligated at one point using a thread to create a closed loop (a and b).

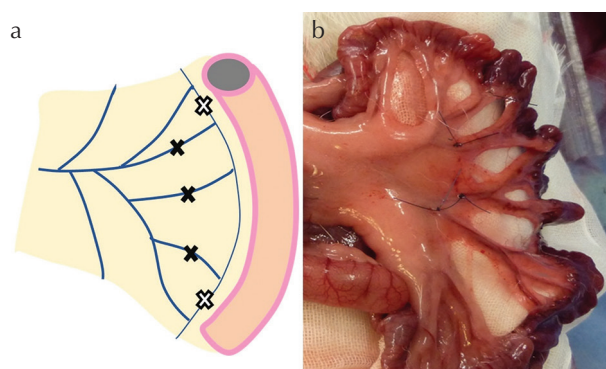


Fig. 2 Surgical procedure to induce a mesenteric venous occlusion (MVO). The three branches of the mesenteric vein and both ends of the marginal vein were ligated using a thread (a and b).

and mesentery outside the body, and waited for 15 min; after that, we placed the small bowel and mesentery back into the abdominal cavity and closed the abdominal wall.

Angiography

The right femoral artery was exposed using the cut-down method, and a 4-Fr introducer sheath (Super sheath, length: 7 cm, Medikit, Tokyo, Japan) was inserted into the aorta. A 4-Fr cobra-shaped catheter (Terumo Clinical Supply, Gifu, Japan) was inserted into the superior mesenteric artery. Angiography was carried out using a fluoroscopic system (Plessart 50 DREX-WIN20P, Canon Medical Systems, Tochigi, Japan) with a tube voltage of 70 kV and a tube current of 50 mA. Angiography via the superior mesenteric artery using 5 mL of iodine contrast medium (370 mg I/mL, Iopamidol 370, Bayer Yakuhin, Osaka, Japan) was performed manually both before and after creating the strangulated SBO (Fig. 3), MVO models (Fig. 4), and sham surgery models. We judged the success in creating the strangulated SBO model by the defect of the mesenteric artery and vein in the ligated lesion, that for the MVO model was judged by depicting the mesenteric artery and the defect of the mesenteric vein, and that for sham surgery group was judged by no change after the surgical procedure compared with the findings before the procedure.

MRI

MRI examinations were performed before and 30 min after creating the mesenteric ischemia models using a 3T scanner (MAGNETOM Verio 3T, Siemens, München, Germany) with a spine matrix coil and a body matrix coil in our experimental facility, which are used for only animals. Axial T_1 -weighted images (T_1 WIs; BLADE), fat-suppressed T_1 WIs (FS- T_1 WIs; volumetric interpolated breath-hold examination; VIBE), T_2 -weighted images (T_2 WIs; BLADE), and fat-suppressed T_2 WIs (FS- T_2 WIs; BLADE) were



Fig. 3 Angiogram of a strangulated small bowel obstruction (SBO) rabbit. Angiogram before the surgical procedure shows all branches of the mesenteric artery and vein (a). Angiogram after the surgical procedure reveals the disappearance of branches in the ligated mesenteric area (b).

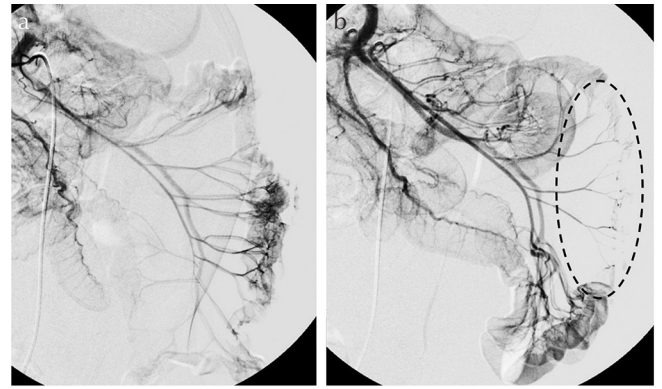


Fig. 4 Angiogram of mesenteric venous occlusion (MVO) rabbit. Angiogram before the surgical procedure shows all branches of the mesenteric artery and vein (a). Angiogram after the surgical procedure depicts the branches of the mesenteric artery but not those of the mesenteric vein (b).

obtained without a breath-gated technique. Their parameters are shown in Table 1. Figure 5 summarizes the protocol in this study.

Imaging analysis

All MR images were reviewed by two radiologists (S.O. and A.I., with 22 and 12 years of experience reading medical images, respectively). First, the thickness of the ischemic bowel wall was measured at the short-axis bowel displaying a circular shape on T_2 WIs by two readers independently because the contrast among lumen, bowel wall, and mesentery is clear on T_2 WIs compared with the other sequences, and the average was accepted as the result. Second, we visually evaluated the signal intensity of the ischemic bowel on all sequences and the mesentery on FS- T_2 WIs in comparison with the normal bowel findings before the surgical procedure, with the intensity classified as low, iso, or high. All decisions were reached by consensus. Third, the signal intensities of the ischemic bowel wall and psoas muscle were measured by two readers independently, and the average was accepted as the result. The signal intensity ratio (SI ratio) was calculated as follows:

$$SI_{\text{ratio}} = \frac{SI_{\text{bowel}}}{SI_{\text{muscle}}}$$

Histopathology

We incised the abdominal wall and recorded the color of the bowel immediately after MRI. Ischemic bowels with 5 cm of non-ischemic tissue on both sides in strangulated SBO and MVO models and an extracted bowel in sham surgery model were excised for microscopic examination. The specimens were stored in 10% formalin for 2 days. The samples were taken in three portions at the center of the ischemic bowel and both borders, including ischemic and non-ischemic bowels. Samples were embedded in paraffin, cut into 3.5- μm sections, and stained with hematoxylin–eosin. Histopathological

Table 1 Magnetic resonance imaging protocol in this study

Parameter	T ₁ WI (BLADE)	FS-T ₁ WI (VIBE)	T ₂ WI (BLADE)	FS-T ₂ WI (BLADE)
Plane	Axial	Axial	Axial	Axial
Breath hold	No	No	No	No
Fat saturation	No	Yes	No	Yes
FOV (mm)	200	200	200	200
Matrix (mm)	256 × 256	256 × 256	256 × 256	256 × 256
Slice thickness (mm)	3	3	3	3
Gap (mm)	0.9	0.9	0.9	0.9
Repetition time (ms)	700	4.89	6400	6930
Echo time (ms)	49	2.47	81	81
Flip angle (°)	140	140	140	140
Averages	1	1	1	1
Scan time	4:51	0:22	3:33	3:50

T₁WI, T₁-weighted image; FS, fat-suppressed; T₂WI, T₂-weighted image; VIBE, volumetric interpolated breath-hold examination.

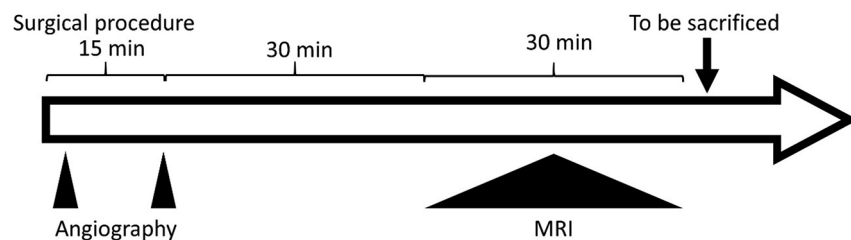


Fig. 5 Summary of the protocol in this study. Angiography was performed before and after the surgical procedures to create acute mesenteric ischemia models. Surgical procedure took 15 min. The MRI scan was started 30 min after angiography. After MRI, the rabbit was sacrificed.

Table 2 Bowel wall thickness in strangulated SBO and MVO models before and after the procedure

	Before procedure	After procedure	Ratio	<i>P</i> -value
Strangulated SBO	1.2222 ± 0.9718	2.2611 ± 0.4586	1.8500	<0.0001*
MVO	1.1822 ± 0.2178	3.1700 ± 0.5491	2.6814	<0.0001*
Sham surgery	1.4550 ± 0.2333	1.3500 ± 0.0849	0.9278	0.7220

Significant difference (**P* < 0.05). SBO, strangulated small bowel obstruction; MVO, mesenteric venous obstruction.

findings were reviewed by one pathologist (K.M. with 17 years of experience in pathological diagnosis) who was blinded to the surgical procedure.

Statistical analysis

Bowel wall thickness and the signal intensity of the bowel wall were compared between the diseased and normal bowels using Student's *t*-test. *P*-values ≤ 0.05 were considered statistically significant. Statistical tests were performed by using SPSS statistics 22 (IBM, Chicago, IL, USA).

Results

Angiography

The mesenteric artery and vein in the closed loop were not depicted on angiogram in all nine strangulated SBO rabbits. The mesenteric artery was depicted in all nine MVO rabbits

on angiogram, but the mesenteric vein was not shown. Both the mesenteric artery and vein were revealed in sham surgery rabbits on angiogram.

MR image

The bowel wall in strangulated SBO rabbits was significantly thicker (2.26 ± 0.46 mm) than that observed before the procedure (1.22 ± 0.97 mm; *P* < 0.0001). Similar findings were also observed for the MVO rabbits (3.17 ± 0.55 vs. 1.18 ± 0.22 mm; *P* < 0.0001); however, there was no significant change in the sham surgery rabbits (1.45 ± 0.23 vs. 1.35 ± 0.08 mm; *P* = 0.7220) (Table 2). The bowel wall was thicker in MVO rabbits than in strangulated SBO rabbits (*P* = 0.0016).

In strangulated SBO rabbits, the ischemic bowel wall exhibited a high signal intensity in six of nine animals on T₁WIs, T₂WIs, and FS-T₁WIs and in eight of nine animals on FS-T₂WIs. The mesentery adjacent to the ischemic bowel

loop displayed a high intensity in all rabbits on FS-T₂WIs (Table 3 and Fig. 6). In MVO rabbits, the ischemic bowel wall displayed a high signal intensity in five of nine animals on T₁WIs and FS-T₁WIs, in six of nine animals on T₂WIs, and in nine animals on FS-T₂WIs. The mesentery adjacent to the ischemic bowel loop demonstrated a high intensity in all cases on FS-T₂WI (Table 4 and Fig. 7). In sham surgery rabbits, the bowel showed an isointensity in both rabbits on every sequence (Fig. 8).

The SI ratio of the bowel wall was significantly higher after each procedure than before the procedure on all sequences in strangulated SBO and MVO models (Tables 5 and 6). FS-T₂WIs displayed the largest difference of the SI ratio between before and after the procedure in the strangulated SBO model. T₁WIs and FS-T₂WIs revealed differences in the SI ratio exceeding 2.0 in the MVO model. On the other hand, there was no significant difference in SI ratio of the bowel wall in sham surgery modes (Table 7).

Histopathology

The color of the ischemic bowel wall changed to wine red in strangulated SBO rabbits (Fig. 9a) and to dark red in MVO

rabbits (Fig. 9b) compared with the findings in the sham surgery rabbits (Fig. 9c). Microscopic analysis revealed massive erosion and mild hemorrhage in the mucosa in strangulated SBO rabbits (Fig. 9d) and severe congestion and hemorrhage in all layers and submucosal edema (Fig. 9e) compared with the finding in sham surgery rabbits (Fig. 9f).

Discussion

Diagnosing mesenteric ischemia using MRI is challenging in clinical practice because of the absence of clinical research.^{22,23} This study assessed the utility of MRI for diagnosing mesenteric ischemia caused by strangulated SBO or MVO. Prior research assessing mesenteric ischemia using MRI was performed in rats,^{16–18} rabbits,^{19,20} and pigs.²¹ Rabbits are easier to handle than pigs based on their body weight and lower expenses. A 7T micro MRI system was used in previous studies using rats,^{16–18} whereas a 3T MRI system, which is employed clinically, was used in this study. We considered rats too small to make strangulated SBO and MVO models by surgical procedure with our skill, leading us to use rabbits.

Strangulated SBO is associated with bowel ischemia, which occurs in approximately 10% of patients with SBO.^{24,25} Strangulated SBO is caused most frequently by post-operative adhesion and occasionally by external or internal hernia, which forms closed-loop bowel obstruction. In the early stage of strangulated SBO, bowel strangulation is caused by impairment of venous return, followed by arterial ischemia. Contrast-enhanced CT reveals C- or U-shaped distended loops, with the mesenteric vessels converging toward the point of obstruction with a fan-shaped mesentery, and the thickened bowel wall exhibits absent or diminished enhancement or hyperenhancement with a target pattern.²⁶

Table 3 The result of visual assessment in the strangulated bowel obstruction model

	Bowel wall				Mesentery
	T ₁ WI	T ₂ WI	FS-T ₁ WI	FS-T ₂ WI	FS-T ₂ WI
Low intensity	1	1	0	0	0
Iso intensity	2	2	3	1	0
High intensity	6	6	6	8	9

T₁WI, T₁-weighted image; FS, fat-suppressed; T₂WI, T₂-weighted image.

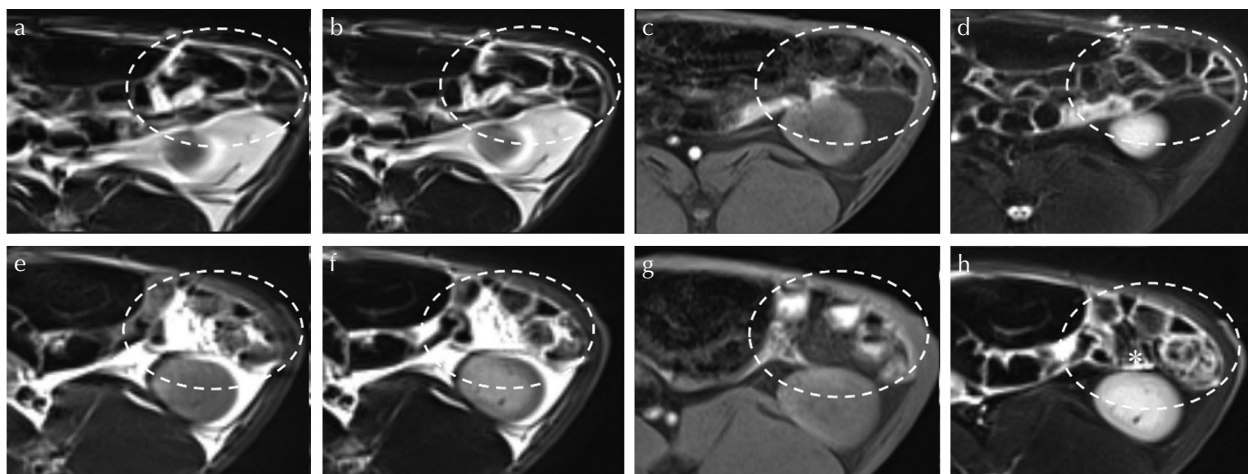


Fig. 6 Magnetic resonance images of the strangulated small bowel obstruction model. At T₁-weighted image (T₁WI) (a), T₂-weighted image (T₂WI) (b), fat-suppressed T₁WI (FS-T₁WI) (c), and FS-T₂WI (d) were obtained from each animal before the surgical procedure. T₁WI (e), T₂WI (f), FS-T₁WI (g), and FS-T₂WI (h) were obtained after the surgical procedure. The signal intensity of the ischemic area due to strangulated small bowel obstruction on all sequences after the surgical procedure (e–h: circle) was higher than that before the procedure (a–d: circle). The bowel wall was thicker after the surgical procedure (e–h: circle) than before the procedure (a–d: circle).

Contrarily, MVO induced by a thrombus accounts for approximately 5% of cases of primary acute mesenteric ischemia.²⁷ Mesenteric venous thrombosis commonly involves the superior mesenteric vein, which prevents venous return from the small bowel and results in bowel wall edema and

subsequent hemorrhagic infarction.²⁸ The bowel wall is markedly thickened with diminished or absent enhancement or hyperenhancement with a target pattern of contrast enhancement on contrast-enhanced CT. Engorgement of the mesenteric vessel, edema in the mesentery, and ascites are observed on CT.^{2,26} The small bowel, with its mesentery at one point, was ligated using a thread to generate a strangulated SBO model, and the three branches of the mesenteric vein and both ends of the marginal vein were ligated using a thread to generate the MVO model as described previously.^{17,18} We considered that the surgical procedures simulated strangulated SBO and mesenteric venous thrombosis in the clinical setting.

Mesenteric ischemia causes inflammatory changes in the bowel wall and mesentery. Diminished arterial and venous blood flow in strangulated SBO causes inflammation because of ischemia, whereas the remaining arterial blood

Table 4 The result of visual assessment in the mesenteric venous occlusion model

	Bowel wall				Mesentery
	T ₁ WI	T ₂ WI	FS-T ₁ WI	FS-T ₂ WI	FS-T ₂ WI
Low intensity	0	0	0	0	0
Iso intensity	4	3	4	0	0
High intensity	5	6	5	9	9

T₁WI, T₁-weighted image; FS, fat-suppressed; T₂WI, T₂-weighted image.

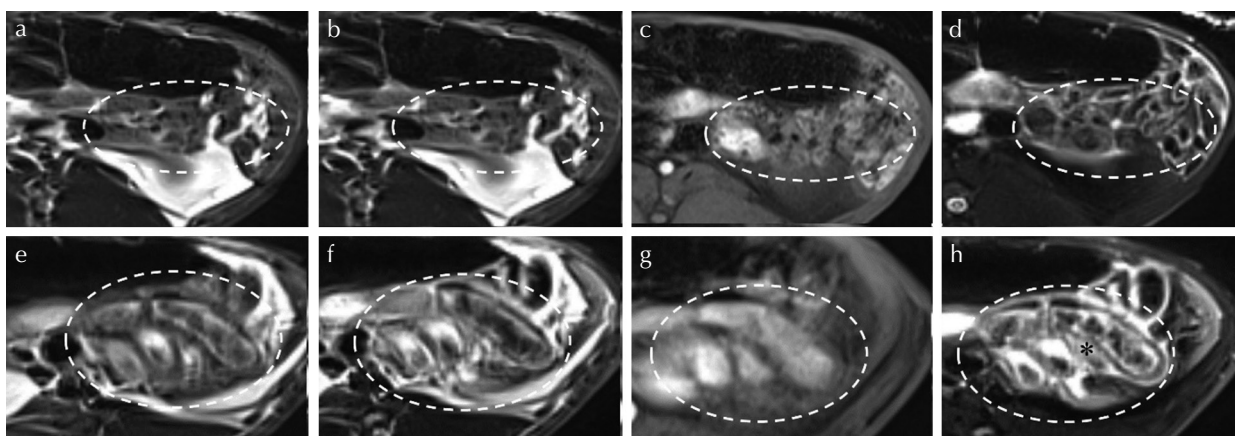


Fig. 7 Magnetic resonance images of the mesenteric venous occlusion model. A T₁-weighted image (T₁WI) (a), T₂-weighted image (T₂WI) (b), fat-suppressed T₁WI (FS-T₁WI) (c), and FS-T₂WI (d) were obtained before the surgical procedure. T₁WI (e), T₂WI (f), FS-T₁WI (g), and FS-T₂WI (h) were obtained after the surgical procedure. The signal intensity of the ischemic area due to strangulated small bowel obstruction on all sequences after the surgical procedure (e–h: circle) was significantly higher than that before the surgical procedure (a–d: circle). The bowel wall was obviously thicker after the surgical procedure (e–h: circle) than before the procedure (a–d: circle).

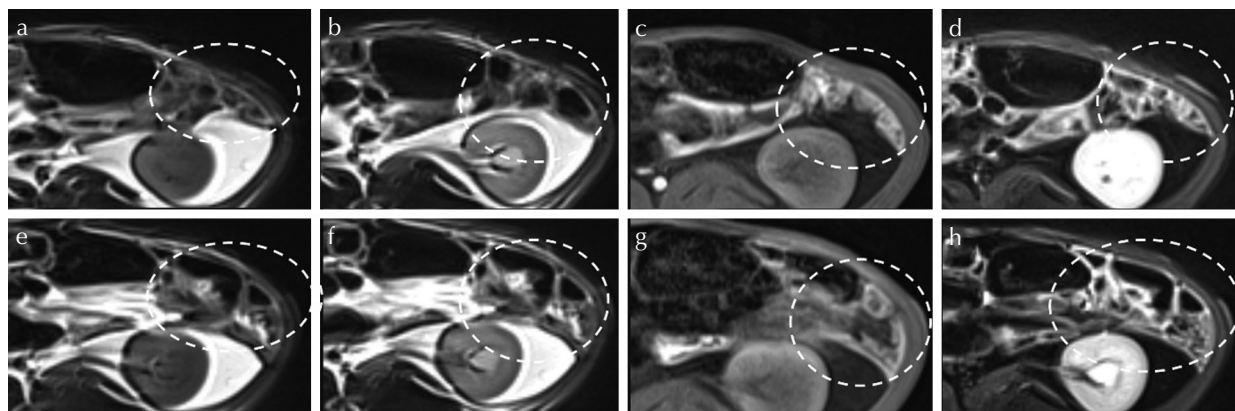


Fig. 8 Magnetic resonance images of the sham surgery. A T₁-weighted image (T₁WI) (a), T₂-weighted image (T₂WI) (b), fat-suppressed T₁WI (FS-T₁WI) (c), and FS-T₂WI (d) were obtained before surgical procedure. T₁WI (e), T₂WI (f), FS-T₁WI (g), and FS-T₂WI (h) were obtained after surgical procedure. Significant change between before (a–d: circle) and after surgical procedure (e–h: circle) is not observed on all sequences.

Table 5 Signal intensity ratio in the strangulated bowel obstruction model

	Before procedure	After procedure	Ratio	P-value
T ₁ WI	2.2517 ± 0.4481	4.0454 ± 0.7823	1.7966	<0.0001*
T ₂ WI	4.2670 ± 1.1609	6.6260 ± 1.4761	1.5528	0.0028*
FS-T ₁ WI	0.9202 ± 0.2243	1.6111 ± 0.3071	1.7508	0.0001*
FS-T ₂ WI	3.7920 ± 1.3508	7.6795 ± 2.4324	2.0252	<0.0001*

Significant difference (**P* < 0.05). T₁WI, T₁-weighted image; FS, fat-suppressed; T₂WI, T₂-weighted image.

Table 6 Signal intensity ratio in the mesenteric venous occlusion model

	Before procedure	After procedure	Ratio	P-value
T ₁ WI	1.9778 ± 0.9966	5.0401 ± 1.6459	2.5483	0.0006*
T ₂ WI	5.1805 ± 2.3498	9.2491 ± 3.9343	1.7854	0.0260*
FS-T ₁ WI	0.8271 ± 0.1578	1.4821 ± 0.3037	1.7919	0.0002*
FS-T ₂ WI	3.7820 ± 1.3508	7.6795 ± 2.4324	2.0305	0.0018*

Significant difference (**P* < 0.05). T₁WI, T₁-weighted image; FS, fat-suppressed; T₂WI, T₂-weighted image.

Table 7 Signal intensity ratio in the sham surgery model

	Before procedure	After procedure	Ratio	P-value
T ₁ WI	2.6523 ± 0.0979	2.9038 ± 0.2976	1.0948	0.5336
T ₂ WI	0.9209 ± 0.3007	1.1096 ± 0.2467	1.2049	0.1273
FS-T ₁ WI	4.0081 ± 0.6560	3.8886 ± 0.5431	0.9702	0.9107
FS-T ₂ WI	4.7799 ± 0.4309	3.8173 ± 0.8289	0.7986	0.4754

T₁WI, T₁-weighted image; FS, fat-suppressed; T₂WI, T₂-weighted image.

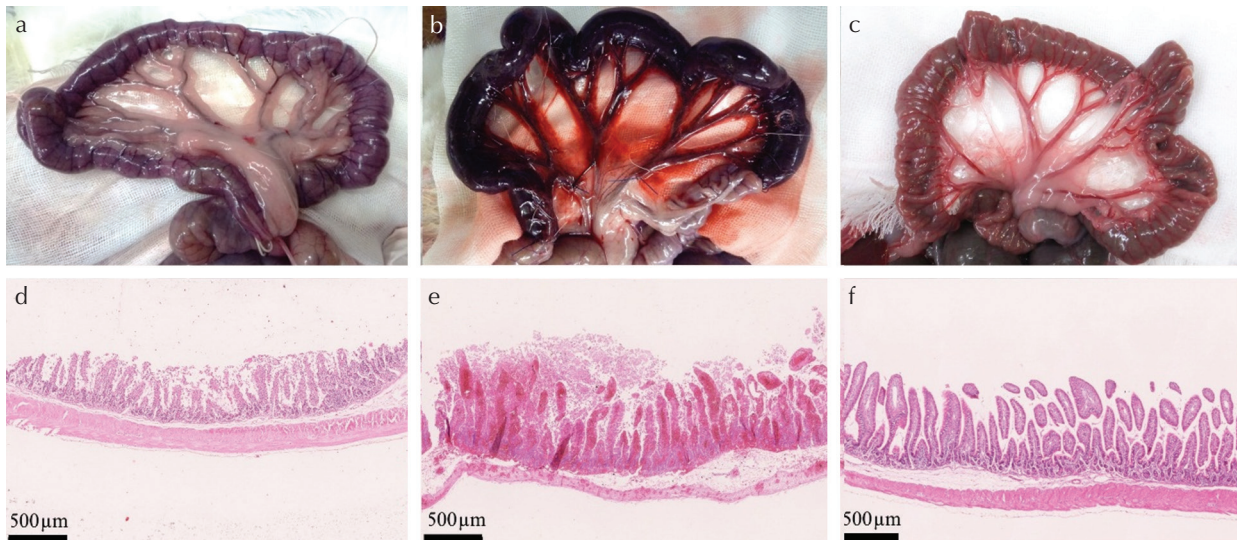


Fig. 9 Macroscopic and microscopic findings of rabbits with strangulated small bowel obstruction (SBO), mesenteric venous occlusion (MVO), and sham surgery. Macroscopically, the ischemic bowel caused by strangulated SBO and MVO was wine red (a) and dark red (b), respectively, compared with the findings of the bowel with sham surgery (c). Microscopically (hematoxylin–eosin stain), massive erosion and mild hemorrhage in the mucosa were noted in strangulated SBO rabbits (d), whereas severe congestion and hemorrhage in all layers and submucosal edema were found in MVO rabbits (e). The findings in rabbits with sham surgery are presented in (f).

supply with disrupted venous return in MVO leads to severe congestion in capillary vessels and edema. These findings explain our result of greater bowel wall thickness in the MVO rabbits.

On the basis of our findings using MRI, the high signal intensity on T_1 WIs and FS- T_1 WIs suggested hemorrhagic infarction, and the high intensity on T_2 WIs and FS- T_2 WIs indicated increasing water levels because of edema, which were supported by histopathological findings. Non-contrast MRI can diagnose mesenteric ischemia resulting from strangulated SBO and MVO based on signal intensity changes, although unlike contrast-enhanced CT, MRI cannot be used to evaluate the blood supply to the mesentery and bowel wall. The study results illustrated that the SI ratio, as a quantitative assessment, was more sensitive than the qualitative assessment. Additionally, FS- T_2 WI was considered the best sequence for detecting mesenteric ischemia.

Previously reported experiments using rats found a high signal intensity in the intestinal wall and little ascites on the TurboRare T_2 sequence 15 min after the surgical procedure for strangulated SBO¹⁸ and 30 min after the surgical procedure for MVO¹⁷. These results were compatible with ours. In clinical research, combined sequences with fast low-angle shot and half-Fourier single-shot turbo spin echo (HASTE) clinically provided greater information about the causes of a disease than CT in bowel obstruction, but not in mesenteric ischemia,²⁹ although cine MRI and low b -value MRI can accurately diagnose mesenteric ischemia by detecting the decreased peristaltic movement of the strangulated small bowel.^{22,23} MRI can evaluate mesenteric venous thrombosis by measuring the oxygen desaturation in the superior mesenteric vein or revealing hypomotility of the small intestine.³⁰

We performed T_1 WIs, T_2 WIs, FS- T_1 WI, and FS- T_2 WIs, which took 30 min of examination time; however, this protocol is not suitable for diagnosis of mesenteric ischemia because acute mesenteric ischemia is required to be diagnosed and treated promptly, and a shorter MRI examination time is desirable. In our result, FS- T_2 WIs in the strangulated SBO model and T_1 WIs and FS- T_2 WIs in the MVO model revealed differences in the SI ratio exceeding 2.0; therefore, we consider that FS- T_2 WI is a priority sequence for acute mesenteric ischemia, and T_1 WI is also helpful in assessing abnormal signal intensity of the bowel wall in MVO in a shorter examination time.

Single-shot T_2 WI sequences such as HASTE are widely used to assess patients with acute abdominal pain because these sequences can obtain images in the lower abdominal region for approximately 20 s with few motion artifacts due to vascular pulsation, respiratory motion, and bowel peristalsis because single-shot T_2 WI with one radiofrequency excitation pulse generates a long train of spin echoes.^{9,12} However, its spatial resolution is lower than that of turbo spin echo T_2 WI because of blurring, especially in small structures possessing a short T_2 relaxation time.^{31–33} Therefore, single-shot T_2 WI is

appropriate for evaluating anatomical structures, but it is not suitable for assessing subtle changes of signal intensity. Contrarily, turbo spin echo T_2 WI provides clearer intensity than single-shot T_2 WI, although the image quality may be low because of motion artifacts. Antispastic agents, including butylscopolamine bromide, decrease the motion artifacts caused by bowel peristalsis, and they are considered to improve the imaging quality of turbo spin echo T_2 WI. However, these agents should not be administered before diagnosis because they are contraindicated in several gastrointestinal diseases causing acute abdominal pain. The BLADE sequence, which acquires k -space data with rotating parallel lines instead of parallel lines, can markedly reduce the motion and magnetic susceptibility artifacts, and it has been used to image the head, breasts, shoulders, upper abdomen, and pelvis with reduced motion artifacts.^{34–38} Thus, we consider the BLADE sequence to be suitable for assessing mesenteric ischemia with subtle changes of signal intensity in the bowel wall.

Limitations

Our study had a few limitations. First, strangulated SBO and MVO models were generated surgically, and the success of surgery was confirmed using angiograms and laparotomy. Strangulated SBO and MVO in the clinical setting gradually diminish blood flow, whereas ischemia suddenly disrupts blood flow in surgically induced strangulated SBO and MVO. Thus, the mesenteric ischemia observed in this study did not precisely mimic the clinical situation, even though MRI could depict abnormal findings in SBO and MVO models 30 min after surgical procedure. Second, in all cases of strangulated SBO and MVO, non-reversible changes were observed in macroscopic and microscopic findings; therefore, it is unclear whether MRI can detect early mesenteric ischemia, which can be reversible. Third, FS- T_1 WIs were obtained using the scanned gradient echo sequence, which can be obtained sooner than spin echo sequences, thus shortening the MRI examination time, which is necessary because general anesthesia can last for approximately 1 h. Therefore, the total examination time of all protocols should be <1 h to reduce unbearable pain and unexpected death. Fourth, MRI is not always available for an emergency setting in many hospitals. Besides, diagnosis of acute mesenteric ischemia with MRI in clinical settings has not been established; therefore, further investigations are needed for clinical application.

Conclusion

Non-contrast MRI allowed the evaluation of mesenteric ischemia caused by strangulated SBO and MVO, and FS- T_2 WIs represented the best modality for depicting high intensity, which denoted edema in the bowel wall and mesentery caused by ischemia. The bowel wall was thicker in MVO than strangulated SBO.

Funding

This study was supported by a grant from the Japanese Society for Abdominal Emergency Medicine.

Acknowledgments

The authors would like to thank Enago (www.enago.jp) for the English language review.

Conflicts of Interest

The authors declare that they have no conflicts of interest.

References

- Wadman M, Syk I, Elmståhl S. Survival after operations for ischaemic bowel disease. *Eur J Surg* 2000; 166:872–877.
- Kanasaki S, Furukawa A, Fumoto K, et al. Acute mesenteric ischemia: multidetector CT findings and endovascular management. *Radiographics* 2018; 38:945–961.
- Wadman M, Block T, Ekberg O, Syk I, Elmståhl S, Acosta S. Impact of MDCT with intravenous contrast on the survival in patients with acute superior mesenteric artery occlusion. *Emerg Radiol* 2010; 17:171–178.
- Mayumi T, Yoshida M, Tazuma S, et al. The practice guidelines for primary care of acute abdomen 2015. *Jpn J Radiol* 2016; 34:80–115.
- Davis PL. Anaphylactoid reactions to the nonvascular administration of water-soluble iodinated contrast media. *AJR Am J Roentgenol* 2015; 204:1140–1145.
- Ray JG, Vermeulen MJ, Bharatha A, Montanera WJ, Park AL. Association between MRI exposure during pregnancy and fetal and childhood outcomes. *JAMA* 2016; 316:952–961.
- Masselli G, Derchi L, McHugo J, et al. Acute abdominal and pelvic pain in pregnancy: ESUR recommendations. *Eur Radiol* 2013; 23:3485–3500.
- Baheti AD, Nicola R, Bennett GL, et al. Magnetic resonance imaging of abdominal and pelvic pain in the pregnant patient. *Magn Reson Imaging Clin N Am* 2016; 24:403–417.
- Eng KA, Abadeh A, Ligocki C, et al. Acute appendicitis: a meta-analysis of the diagnostic accuracy of US, CT, and MRI as second-line imaging tests after an initial US. *Radiology* 2018; 288:717–727.
- Repplinger MD, Pickhardt PJ, Robbins JB, et al. Prospective comparison of the diagnostic accuracy of MR imaging versus CT for acute appendicitis. *Radiology* 2018; 288:467–475.
- Kinner S, Pickhardt PJ, Riedesel EL, et al. Diagnostic accuracy of MRI versus CT for the evaluation of acute appendicitis in children and young adults. *AJR Am J Roentgenol* 2017; 209:911–919.
- Petkovska I, Martin DR, Covington ME, et al. Accuracy of unenhanced MR imaging in the detection of acute appendicitis: single-institution clinical performance review. *Radiology* 2016; 279:451–460.
- Byott S, Harris S. Rapid acquisition axial and coronal T₂ HASTE MR in the evaluation of acute abdominal pain. *Eur J Radiol* 2016; 85:286–290.
- Yu HS, Gupta A, Soto JA, LeBedis C. Emergency abdominal MRI: current uses and trends. *Br J Radiol* 2016; 89:20150804.
- Ditkofsky NG, Singh A, Avery L, Novelline RA. The role of emergency MRI in the setting of acute abdominal pain. *Emerg Radiol* 2014; 21:615–624.
- Berritto D, Somma F, Landi N, et al. Seven-Tesla micro-MRI in early detection of acute arterial ischaemia: evolution of findings in an in vivo rat model. *Radiol Med* 2011; 116:829–841.
- Somma F, Berritto D, Iacobellis F, et al. 7T μ MRI of mesenteric venous ischemia in a rat model: timing of the appearance of findings. *Magn Reson Imaging* 2013; 31:408–413.
- Berritto D, Iacobellis F, Belfiore MP, Rossi C, Saba L, Grassi R. Early MRI findings of small bowel obstruction: an experimental study in rats. *Radiol Med* 2014; 119:377–383.
- Kaufman AJ, Tarr RW, Holburn GE, McCurdy M, Partain CL, James AE. Magnetic resonance imaging of ischemic bowel in rabbit model. *Invest Radiol* 1988; 23:93–97.
- Park A, Towner RA, Langer JC. Diagnosis of persistent intestinal ischemia in the rabbit using proton magnetic resonance imaging. *J Invest Surg* 1994; 7:485–492.
- Bruhn RS, Distelmaier MS, Hellmann-Sokolis M, Naami A, Kuhl CK, Hohl C. Early detection of acute mesenteric ischemia using diffusion-weighted 3.0-T magnetic resonance imaging in a porcine model. *Invest Radiol* 2013; 48:231–237.
- Takahara T, Kwee TC, Haradome H, et al. Peristalsis gap sign at cine magnetic resonance imaging for diagnosing strangulated small bowel obstruction: feasibility study. *Jpn J Radiol* 2011; 29:11–18.
- Takahara T, Kwee TC, Sadahiro S, et al. Low b-value diffusion-weighted imaging for diagnosing strangulated small bowel obstruction: a feasibility study. *J Magn Reson Imaging* 2011; 34:1117–1124.
- Furukawa A, Yamasaki M, Furuichi K, et al. Helical CT in the diagnosis of small bowel obstruction. *Radiographics* 2001; 21:341–355.
- Furukawa A, Yamasaki M, Takahashi M, et al. CT diagnosis of small bowel obstruction: scanning technique, interpretation and role in the diagnosis. *Semin ultrasound CT MR* 2003; 24:336–352.
- Furukawa A, Kanasaki S, Kono N, et al. CT diagnosis of acute mesenteric ischemia from various causes. *AJR Am J Roentgenol* 2009; 192:408–416.
- Shatzel JJ, O'Donnell M, Olson SR, et al. Venous thrombosis in unusual sites: a practical review for the hematologist. *Eur J Haematol* 2019; 102:53–62.
- Kumar S, Sarr MG, Kamath PS. Mesenteric venous thrombosis. *N Eng J Med* 2001; 345:1683–1688.
- Kim JH, Ha HK, Sohn MJ, et al. Usefulness of MR imaging for diseases of the small intestine: comparison with CT. *Korean J Radiol* 2000; 1:43–50.
- Bradbury MS, Kavanagh PV, Bechtold RE, et al. Mesenteric venous thrombosis diagnosis and noninvasive imaging. *Radiographics* 2002; 22:527–541.
- Listerud J, Einstein S, Outwater E, Kressel HY. First principles of fast spin echo. *Magn Reson Q* 1992; 8:199–244.
- Chung HW, Chen CY, Zimmerman RA, Lee KW, Lee CC, Chin SC. T₂-Weighted fast MR imaging with true FISP

- versus HASTE: comparative efficacy in the evaluation of normal fetal brain maturation. *AJR Am J Roentgenol* 2000; 175:1375–1380.
33. Zhang L, Kholmovski EG, Guo J, Choi SE, Morrell GR, Parker DL. HASTE sequence with parallel acquisition and T2 decay compensation: application to carotid artery imaging. *Magn Reson Imaging* 2009; 27:13–22.
 34. Mavroidis P, Giankou E, Tsirikia A, et al. Brain imaging: comparison of T1W FLAIR BLADE with conventional T1W SE. *Magn Reson Imaging* 2017; 37:234–242.
 35. Junping W, Tongguo S, Yunting Z, Chunshui Y, Renju B. Discrimination of axillary metastatic from nonmetastatic lymph nodes with PROPELLER diffusion-weighted MR imaging in a metastatic breast cancer model and its correlation with cellularity. *J Magn Reson Imaging* 2012; 36:624–631.
 36. Lavdas E, Vlychou M, Zaloni E, et al. Elimination of motion and pulsation artifacts using BLADE sequences in shoulder MR imaging. *Skeletal Radiol* 2015; 44:1619–1626.
 37. Zhang L, Tian C, Wang P, et al. Comparative study of image quality between axial T₂-weighted BLADE and turbo spin-echo MRI of the upper abdomen on 3.0 T. *Jpn J Radiol* 2015; 33:585–590.
 38. Lane BF, Vandermeer FQ, Oz RC, Irwin EW, McMillan AB, Wong-You-Cheong JJ. Comparison of sagittal T2-weighted BLADE and fast spin-echo MRI of the female pelvis for motion artifact and lesion detection. *AJR Am J Roentgenol* 2011; 197:W307–W313.